T. TAŃSKI*,#, K. LABISZ*, M. KRUPIŃSKI*, K. LUKASZKOWICZ*, Ł. KRZEMIŃSKI*

STRUCTURE AND PROPERTIES OF DIAMOND-LIKE CARBON FILMS DEPOSITED BY PACVD TECHNIQUE ON LIGHT ALLOYS

The investigations presented in this paper describe surface treatment performed on samples of heat-treated cast magnesium and aluminium alloy. The structure and chemical composition as well as the functional and mechanical properties of the obtained gradient/monolithic films were analysed by high resolution transmission electron microscopy and scanning electron microscopy, Raman spectroscopy, the ball-on-disk tribotester and scratch testing. Moreover, investigation of the electrochemical corrosion behaviour of the samples was carried out by means of potentiodynamic polarisation curves in 1-M NaCl solution. The coatings produced by chemical vapour deposition did not reveal any delamination or defects and they adhere closely to the substrate. The coating thickness was in a range of up to 2.5 microns. Investigations using Raman spectra of the DLC films confirmed a multiphase character of the diamond-like carbon layer, revealing the sp^2 and sp^3 electron hybridisation responsible for both the hardness and the friction coefficient. The best wear resistance test results were obtained for the magnesium alloy substrate - AZ61, for which the measured value of the friction path length was equal to 630 m.

Keywords: DLC; coating; PACVD; magnesium; HRTEM.

1. Introduction

Since the 1990s, the world has seen a rapid growth in the application of light metals and their alloys in almost every field, particularly the automobile industry. This sector generally relies on innovative constructional solutions as well as modern materials, which directly influence mass, performance and fuel consumption [1-3]. One of the basic groups of materials, which allow the realisation of the mentioned tasks, are magnesium and aluminium alloys. Deposition of hard layers of nitrides, carbides or oxides on surfaces of engineering materials using physical vapour deposition (PVD) and chemical vapour deposition (CVD) processes is a promising way of extending the functional elements' life [4-15, 18-20].

One of the most attractive options is thin film deposition using low temperature plasma techniques, such as plasma assisted chemical vapour deposition (PACVD) and plasma enhanced chemical vapour deposition (PECVD), which enable the deposition of non-equilibrium phases and better control of the chemical composition and purity of coatings than in the case of conventional CVD techniques; they also enable the production of hard surface layers or layers with special properties in terms of surface and volume (e.g. protective, corrosion, tribological). One of the problems occurring during the deposition is the presence of some metal droplets deposited on the surface, which is associated with the quality of the supplied voltage and self-bias. Self-bias shows the interdependence deposition rate as a function of the self-bias voltage and as a function of the ion current for films deposited by PACVD, respectively. An increase in the deposition rates was observed for DLC films deposited by PACVD. This behaviour can be explained by the higher power input needed to achieve the desired self-bias voltage, and consequently, the more efficient plasma dissociation. The low deposition temperature of the layers is achieved with the PACVD method by plasma excitation of the gas mixture particles to energy level, thus ensuring thermal excitation [9-15]. Lowering the pressure increases the diffusivity of gasses, which results in faster formation of the diffusion layer at lower partial pressures of the reactants, and a lower temperature. In addition, a significant temperature reduction by application of thin layers enables the use of PACVD, which is impossible to obtain with the low temperature CVD technique for substrates, including cast magnesium and aluminium alloys.

The PACVD method is often used for carbon-based coatings, particularly diamond-like carbon coatings (DLC). DLC coatings have an amorphous structure, but also have some of the features of a natural diamond. DLC coatings consist of a mixture of amorphous as well as fine-grained carbon. DLC coatings reveal electron hybridisation sp^3, sp^2 and sp^1. In the sp^3 configuration, as in diamond, a carbon atom has four valence electrons and each is assigned to a tetrahedrally directed sp^3 orbital, which makes a strong bond with the next atom; this material has high functional properties. The amount of the crystalline phase, revealing the sp^3 hybridisation in the DLC coating, is crucial for the choice of method and the conditions for its application [14-17].

The sp^2 phase, as in graphite, has a strong intra-layer σ bonding and weak van der Waals bonding between the

* INSTITUTE OF ENGINEERING MATERIALS AND BIOMATERIALS, FACULTY OF MECHANICAL ENGINEERING, SILESIAN UNIVERSITY OF TECHNOLOGY, 18A KONARSKIEGO STR., 44-100 GLIWICE, POLAND

Corresponding author: tomasz.tanski@polsl.pl

layers, ensuring a low-friction coefficient of the coatings and good electrical conductivity. The chemical inactivity, high hardness and wear resistance decide the sp^3 phase. Therefore, thin diamond carbon DLC coatings have high hardness, high corrosion and tribological resistance as well as high electrical resistivity. These properties are achieved in an isotropic disordered film with no grain boundaries and are much cheaper to produce than diamond itself. From the tribological perspective, the application of DLC coatings is useful for sliding joints operating under limited lubrication and dry friction conditions. Control of film properties is strongly dependent on the characteristics of the chosen deposition technique. This determined the originality of the present work based on the use of chemical vapour deposition technology in order to improve the mechanical and functional surface properties of the most popular structural metals, such as light magnesium and aluminium alloys. The mechanical properties of DLC coatings are of great importance because of the possible use of DLC as a protective coating. There are also some disadvantages of the DLC films concerning their intrinsic stress and thermal stability [14-17].

Therefore, it is important to investigate coating structures that also consist of the amorphous phase; e.g. tetrahedral amorphous carbon (ta-C) containing films with sp^2-rich surface layers. The aim of this work was to obtain the best possible hybrid coatings consisting of a gradient transition layer, with a continuous change of one component reaching from the substrate to the surface top, as well as an outer coating by using the PACVD process on the surface of cast magnesium and aluminium alloys. The main reason was to increase the low stiffness of the substrate material, while simultaneously providing the highest possible adhesion of the coating to the substrate, leading to an increase of the wear resistance and a sufficiently high resistance to aggressive agents, as well as the relaxation of tensions between the coating and the substrate material.

2. Experimental procedure

The investigations were carried out on test pieces of magnesium and aluminium alloys (Table 1). The dimensions of the investigated samples used for coating deposition were 17×17×10 mm. Before the deposition of coatings, the substrate was thinned and polished. The average roughness coefficient after polishing was 0.30 for both materials. The samples were cleaned by washing and rinsing in ultrasonic and cascading cleaners, and dried in a stream of hot air. The DLC coating was produced by the PACVD process (Table 2).

The substrates were cleaned by argon ion sputtering at 2 Pa for 20 min with a bias step-wise changing voltage of 800 V and 200 V. In order to obtain the high adhesion of a low friction layer, a titanium-based metallic transition layer was applied with the arc method, and a DLC coating of the a-C:H:Si (amorphous carbon-hydrogen-silicon) and a-C:H (amorphous carbon-hydrogen) layer with the PACVD method.

Examinations of the thin film's microstructure and phase identification were performed with a high-resolution transmission electron microscope Titan 80-300 from FEI with the STEM scanning mode. The thin cross-section lamellas for TEM observations were prepared by the focused ion beam (FIB) technique using the Quanta 200i instrument with gallium ions.

Adhesion tests were done with the scratch test on a CSEM REVETEST device by moving the diamond indenter along the examined surface with a gradually increasing load: from 0 to 100 N; load increase rate (dL/dt): 10 kG/min; speed of indenter's sliding (dx/dt): 0,01 m/min and acoustic emission detector. The device registered the friction force, friction coefficient, indenter penetration depth and acoustic emission along the scratch track.

The microhardness tests of the coatings were done with a SHIMADZU DUH 202 ultra-microhardness tester. The measurements were done with a load of 10 mN in order to eliminate the substrate's influence on the coating hardness.

TABLE 1

Chemical composition of investigated alloys

Type of material	Mass concentration of the elements, wt. %							
	Al	Zn	Mn	Si	Mg	Fe	Cu	Rest
Magnesium alloy-AZ91	9.09	0.77	0.21	0.04	89.8	0.011	-	0.079
Magnesium alloy-AZ61	5.92	0.49	0.15	0.04	93.3	0.007	-	0.093
Aluminium alloy-AlSi9Cu4	85.4	0.05	0.01	9.27	0.28	0.34	4.64	0.01
Aluminium alloy-AlSi9Cu	88.86	0.16	0.37	9.1	0.27	0.18	1.05	0.01

TABLE 2

Deposition parameters of the investigated coating

Parameters	Coating type
	DLC
Base pressure [Pa]	$1×10^{-3}$
Working pressure [Pa]	2
Acetylene flow rate [sccm]	230
Substrate bias voltage [V]	500
Process temperature [°C]	<180

Wear resistance investigations were performed with the ball-on-disk method in dry friction conditions and in a horizontal settlement of the rotation axis of the disk. A tungsten carbide ball with a diameter of 3 mm was used as a counterpart. The tests were performed at room temperature for a defined time period and under the following conditions: load F_N - 5N, rotation of the disk - 200 rpm, wear radius - 2.5 mm, shift rate - 0.05 m/s.

The specimens were tested on a Raman spectroscope, coupled with a light microscope; a laser with a wavelength of 514 nm was used for observation.

Pitting corrosion resistance of the analysed alloys was assessed with the potentiodynamic electrochemical method (direct current), based on an anodic polarisation curve. The corrosive agent was a 1 M NaCl solution. The measurements were performed at room temperature, 20 minutes after the first contact of the investigated material with the electrolyte, by potential change of 120 mV/min. The surface area of the tested samples of the cast magnesium alloys was equal to 0.5 cm^2.

3. Discussion of experimental results

The results of the tests obtained using the transmission electron microscope confirmed the amorphous character of a low-friction DLC layer. The electron diffraction patterns showed a considerable broadening of the diffraction rings (Fig. 1).

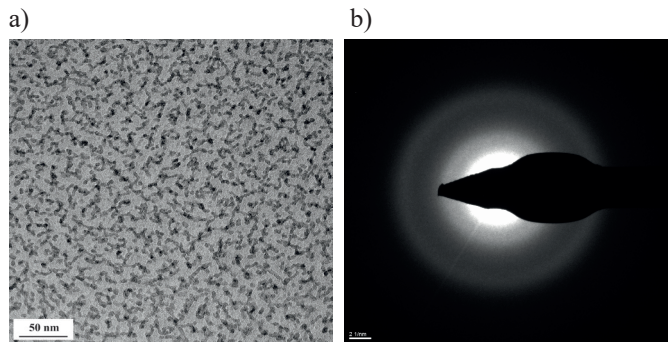a)   b)

Fig. 1. Structure of DLC layer: a) image in the bright field, b) SAED pattern with the area as in a)

The DLC layer, starting with about 800 nm, showed an increased concentration of Si and two sublayers were visible (Fig. 2a). An increase in the Si concentration and a decrease of the C concentration occurred in the first layer and were maintained at a constant level in the other one. They were both amorphous and differentiable on a diffraction image (Fig. 2b). Information about the mass and atomic concentration of individual elements in the microareas of the sublayers was acquired as a result of an X-ray quantitative WDS microanalysis (Table 3).

On the basis of the performed investigations on the scanning electron microscope, it was possible to confirm the occurrence of micro-particles in the shape of droplets on the surface of the investigated coatings. There were also some hollows, probably formed when the solidified droplets broke off after the CVD process had been completed (Figures 5 to 8). The occurrence of such particles is not good for the quality of the surface. The droplets observed in SEM were noticeably different in terms of size and shape (regular and irregular shape, slightly flat). One of the reasons is the high-voltage quality on the driven electrode, the best way to ensure a high stability is to use an oscilloscope, well-grounded to the chamber. This could act as regulation of the voltage noise and will be your self-bias. Working at low self-bias voltages that are higher than 100 V will have to take care of the plasma potential to determine the ion bombardment energy, the first reasonable value should be +/- 15 V. An appropriate - high-inductance, followed by a voltage divider, could be the proper solution to avoid the metal drops on the surface. The inductance would filter out the noise and only let the DC average value pass through. The voltage divider has to have high impedance, which is also not favourable for a high voltage and it cannot be driven by too much current, since this current will modify the self-bias, influencing the plasma carrier balance, which - as assumed - will help to achieve an appropriate quality of the PACVD surface.
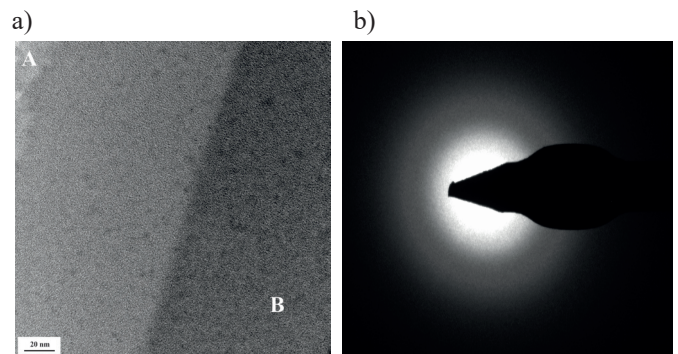
a)   b)

Fig. 3. a) TEM image of DLC sublayers, b) SAED pattern

TABLE 3

Results of quantitative analysis of chemical composition of DLC layers in Fig. 3

Element analysed	Concentration, %	
	mass concentration	atomic concentration
point A		
C	97.9	98.6
O	1.3	1.0
Si	0.8	0.4
point B		
C	63.9	79.7
O	2.6	2.5
Si	33.5	17.8

The produced coatings of the Ti/DLC/DLC type layers revealed the presence of a sharply visible transition zone placed between the coating and the substrate. During microstructure investigations with a scanning electron microscope, it was confirmed that, in the coating, there were no pores or other defects like cracks or discontinuities. A considerable adhesion was found for the Ti-interlayer, which is of uniform thickness and quality spread over the whole visible investigated area in Fig. 7 and 8, both for the magnesium as well as aluminium cast alloy. The only difference is the thickness and intensity of the interlayer-zone, which is wider in cast of magnesium and sharply - almost abruptly - ending in case of the AlSi9Cu alloy.
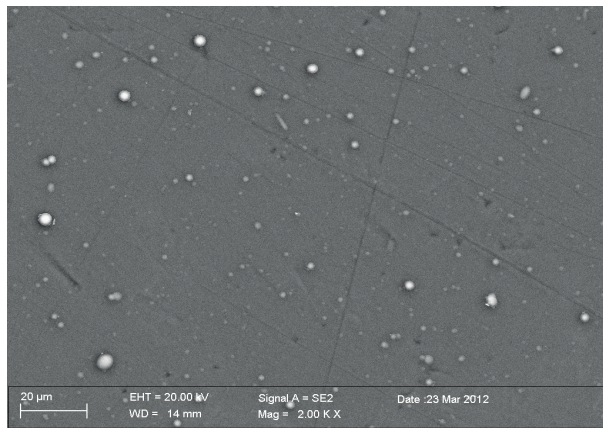
Fig. 5. Surface topography of the DLC coating deposited onto AlSi9Cu substrate
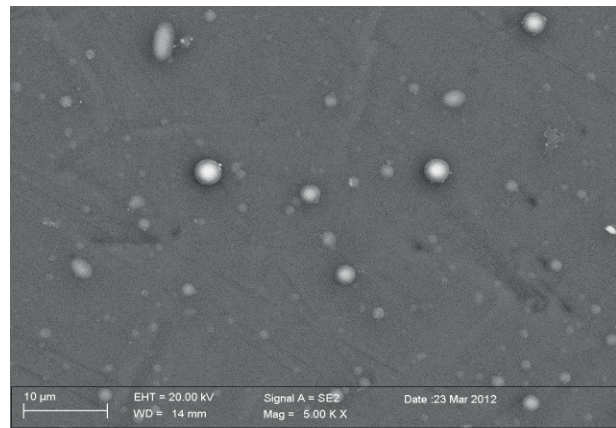

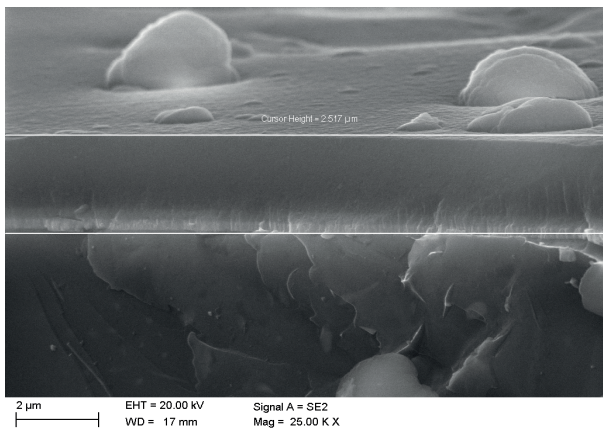Fig. 6. Surface topography of the DLC coating deposited onto AlSi9Cu substrate

Fig. 7. Cross-section SEM images of the Ti/DLC/DLC coating deposited onto the AZ91 substrate
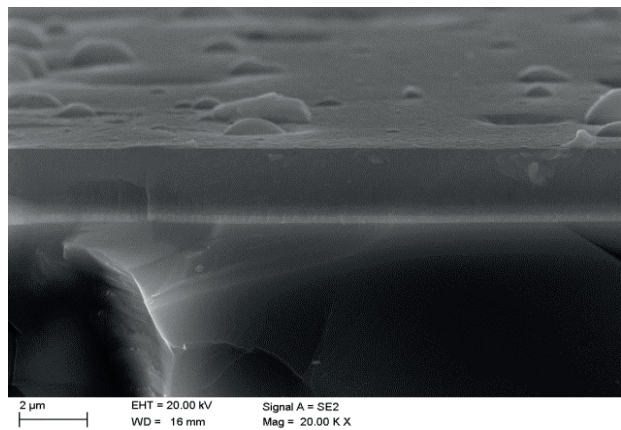

Fig. 8. Cross-section SEM images of the Ti/DLC/DLC coating deposited onto the AlSi9Cu substrate

Only small amounts of the above-described defects were present in the coating, which occurred spontaneously and had no significant influence on the wear resistance or other functional surface properties of the pair coating substrate, such as adhesion, wettability or corrosion resistance. Investigations carried out by scanning electron microscopy determined the thickness of the produced coating, which was in a range of up to 2.5 microns.

X-ray microanalysis using the qualitative energy spectrometer EDS confirmed the presence of major alloying elements Al, Si, Cu, Ti, C, as compounds of the investigated alloys (in this case cast aluminium) as well of the coatings (Figure 9).

In order to perform a complete identification of coatings of the Ti/DLC/DLC type obtained by the PACVD method, investigations were performed using the Raman spectrometer, which confirmed that the coatings consisted of poorly ordered carbon material consisting of amorphous material, in which small graphite crystallites were distributed. The Raman spectra for DLC films presented two overlapping bands known as the D and G bands. While the D band, appearing approximately at 1360 cm^{-1} to 1370 cm^{-1}, is derived from the relaxation of the D6h point group symmetry of finite graphite crystallites, which allows forbidden modes to show Raman activity, the G band, appearing approximately at 1550 cm^{-1} to 1560 cm^{-1}, is associated with the optically allowed E2g mode zone centre of crystalline graphite.

The obtained Raman spectrum was presented as the sum of two Lorentz curves and one Gaussian curve, according to Raman shift values equal to about 1370 cm^{-1} (D1 band), 1560 cm^{-1} (D3 band) and 1560 cm^{-1} (G band) (Figure 10). The spectra can be adjusted by two Gaussian lines. The ratio of intensity of the G and D peaks, the G band, peak position (ωG), ID/IG, and the full width of the G peak (ΓG) at half maximum, is obtained as a function of the ion current and as a function of the self-bias voltages, for the optimal parameters. All graphics showed the same behaviour. An increase of the ID/IG ratio, together with the shift of the G band's peak position towards higher frequencies, accompanied by a reduction of the full width at half maximum of the G peak, is usually interpreted in terms of an increase of graphitic domain size. The results show a process of graphitisation, wherein in accordance with C. Casiraghi, these a-C:H films contain less than 20 at.% and exhibit a high sp^2 content. The D1/G ratio was an ordering indices structure of carbon of the analysed material. The D3 peak confirmed the occurrence of the non-crystalline phases.
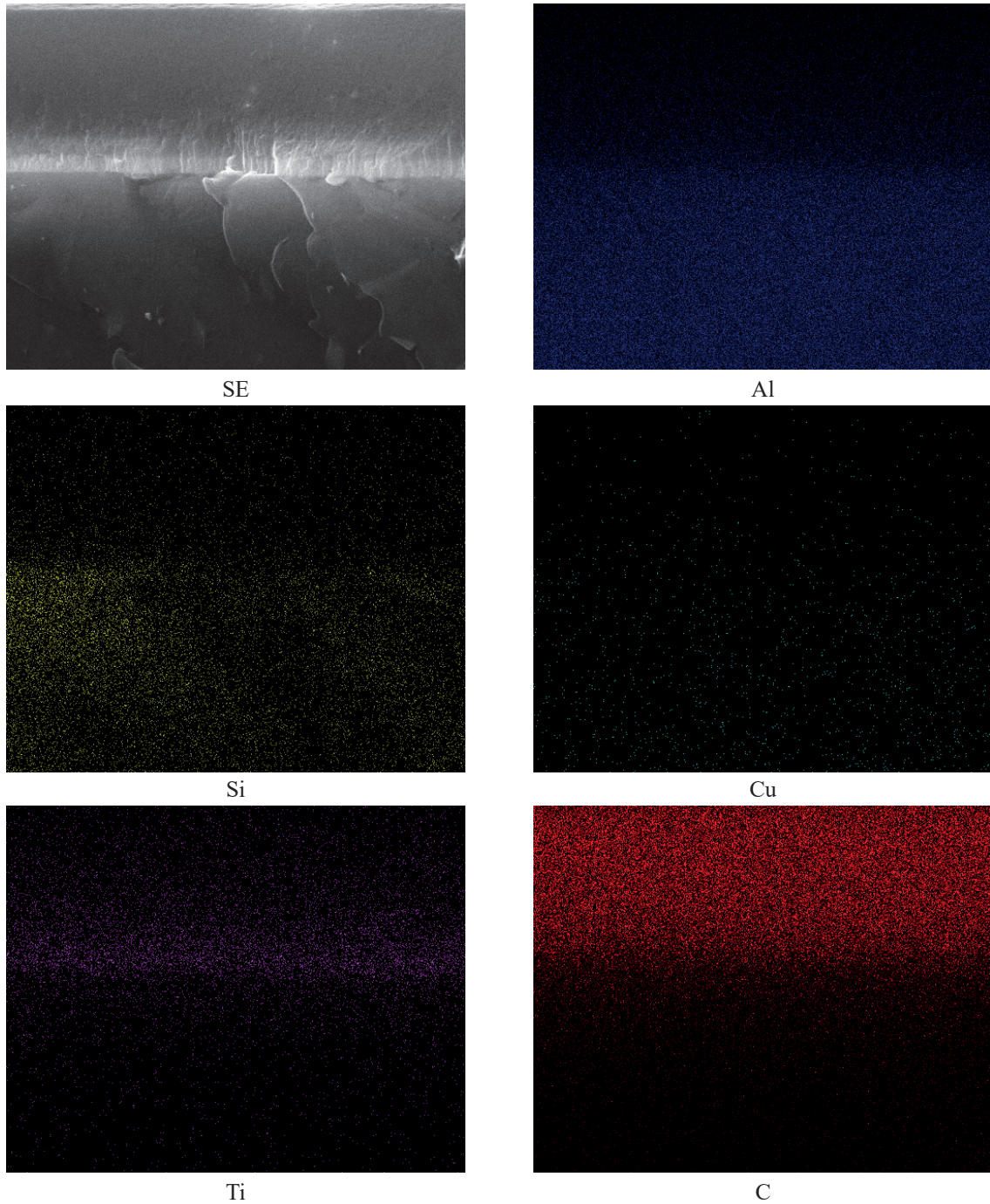
Fig. 9. The area analysis of chemical elements of the Ti/DLC/DLC coating and the aluminium (AlSi9Cu4) substrate: image of the secondary electrons and maps of elements' distribution
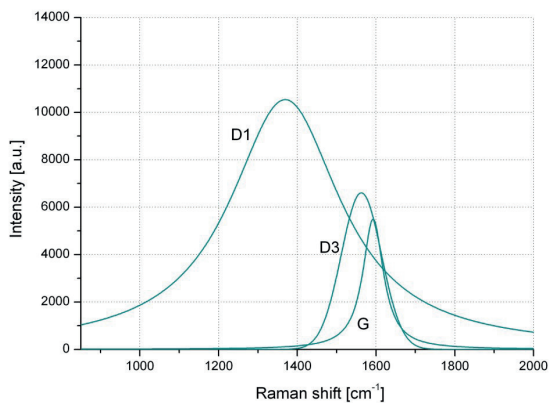

Fig. 10. Raman spectra of the DLC films deposited on magnesium alloy

The critical loads LC1 and LC2 were determined by the scratch test method. The first critical load LC1 corresponds to the point at which first damage is observed; the first damage means: the first appearance of microcraking, surface flaking outside or inside the track without any exposure of the substrate material-the first cohesion-related failure event (Figs. 11a, 12a).When referring to the obtained values, it can be concluded that the LC1 parameter is accountable for the prime small jump on the emitted acoustic signal, whereas the second critical load LC2 is the value and the starting point at which entire delamination of the test coating occurs. Entire delamination should be understood to include the first appearance of any cracking, chipping, spallation and delamination outside the scratch track, which reveals the substrate material (Figures
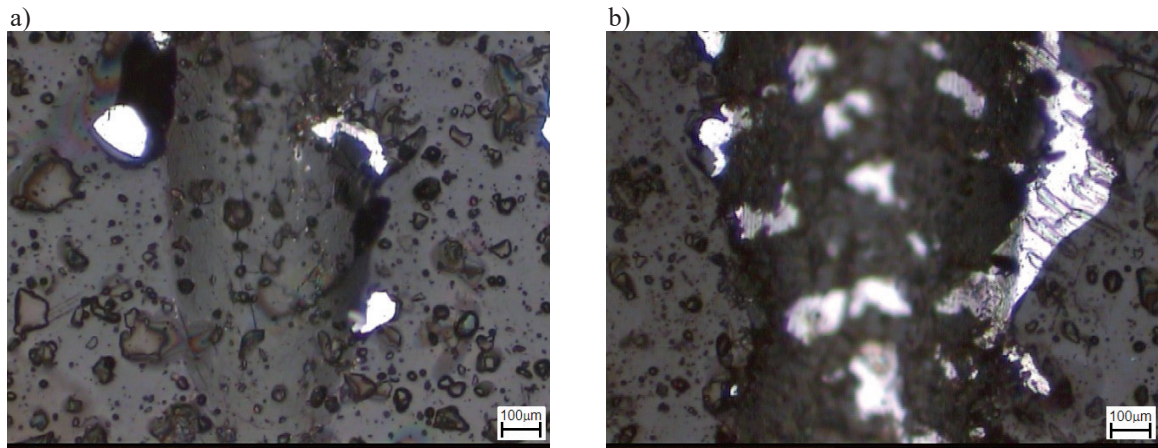
a)

b)

Fig.11. Scratch damage pictures of the Ti/DLC/DLC coating on AlSi9Cu4 substrate at: (a) LC1, (b) LC2
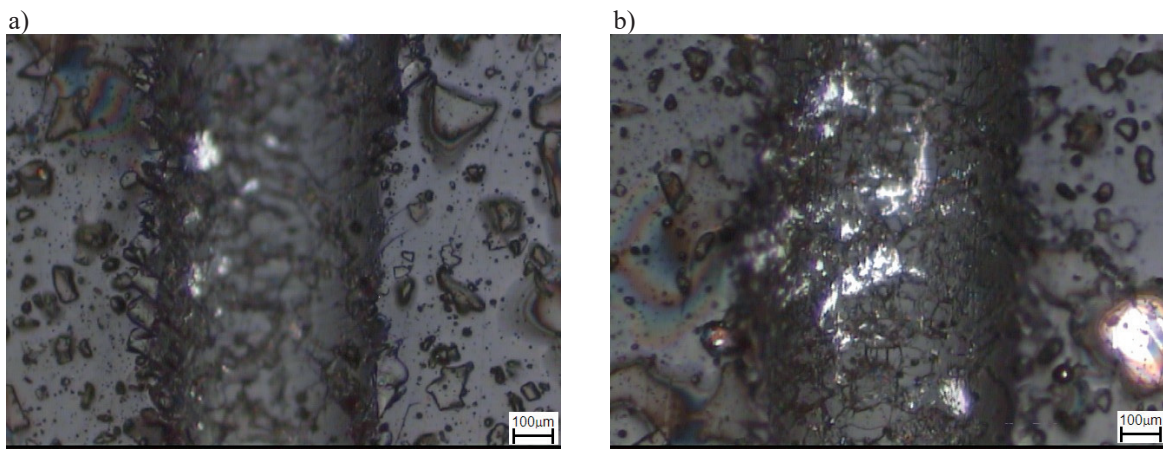
a)

b)

Fig. 12. Scratch failure pictures of the Ti/DLC/DLC coating on AZ91 substrate at: (a) LC1, (b) LC2

11b and 12b). The delamination of the layer is physically determined as the acoustic emissions at the friction force that are louder.

Investigation results concerning the mechanical properties, including microhardness, are compared and presented in Table 4, where it can be seen that the highest measured critical load of the L_{C1} parameter is 7 N and the L_{C2} parameter is 19 N, and that the best adhesion of the coating to the substrate was obtained for the AZ91 magnesium alloy. For the aluminium alloy AlSi9Cu coated with the same investigated coating the L_{C1} and L_{C2}, the lowest achieved values were 6 N and 10 N, respectively.

The hardness of the deposited coatings correlates mainly with their wear resistance within a range of about 2000 HV (Table 4). However, it is not always important for the friction pair to increase the surface hardness; a good example of this is the self-lubricating DLC coating, which reduces the friction force (friction coefficient); therefore, it protects the surface against wear. In accordance with the applied load of 5 N, the average friction coefficient of DLC coatings obtained with the sliding speed of 0.05 m/s was in the range of 0.08 to 0.14 (Table 4, Figure 13), respectively - one grade lower than the friction coefficient of the other investigated coatings.

TABLE 4

Summary results of the mechanical properties

Substrate	Microhardness [HV]	L_{C1} [N]	L_{C2} [N]	Friction coefficient	Sliding distance [m]
Ti/DLC/DLC					
AZ61	1979.5	6	17	0.09-0.12	630
AZ91	1983.5	7	19	0.11-0.14	540
AlSi9Cu	1989.6	3	9	0.13-0.14	392
AlSi9Cu4	1974.8	3.5	10	0.08-0.09	430

This condition is typical of DLC coatings and it acts in the abrasion process like a lubricant, depositing on the counter sample. Moreover, high wear speed and heat accumulation result in an easier formation of a self-lubricating layer, which further results in a lower friction coefficient [16-17]. During the tribological resistance investigation of the produced coatings, graphs were recorded showing the friction coefficient of and/or presenting the counter specimen displacement in the vertical axis, depending on the rotation speed or the path done by a counterpart until the coating was damaged. All of the measurement data presented in the form of a curve reveal a similar shape; this characteristic depends on the number of

cycles as well as on the friction path length. The entire curve can be divided into two different parts with diverse characteristics, showing the nature of the measurement process (Figure 13). In the first part, rapid increase of the friction coefficient with an increase of the friction path was observed. It is assumed that this is not a steady state. In the other part, and in relation to the steady stable state of the friction test, the friction coefficient changed very rapidly during the investigation, a phenomenon caused by surface spalling of the investigated sample as well as surface spalling in the counterpart. This mechanism involves a gradual build-up of stress around the structural defect of the surface layer associated with the cyclic contact stresses and the formation of micro cracks.
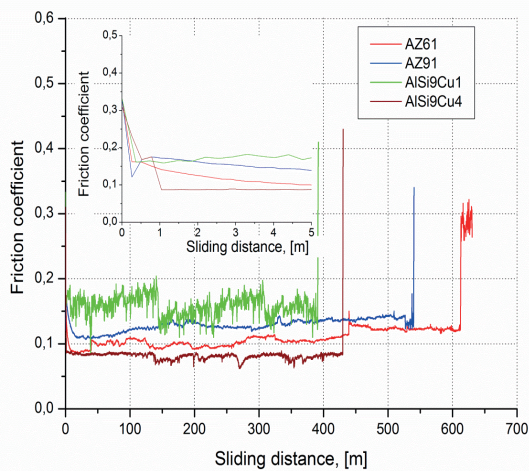

Fig. 13. Dependence of the friction coefficient on the friction path of counter specimen measured for Ti/DLC/DLC coatings deposited on the substrate of cast magnesium and aluminium alloys.

The best results for the wear resistance measurement, with the friction path length of the counterpart until the coating penetration used as a benchmark, were obtained for the AZ61 magnesium alloy substrate and were equal to 630 m (Table 4, Figure 13).

For the purpose of establishing the impact of the surface processing on the corrosion resistance of the cast alloys Mg-Al-Zn and Al-Si-Cu, corrosion tests with the use of the electrochemical potential-dynamic method were performed. The corrosion resistance is not solely dependent on surface roughness, but also on other factors, such as coating materials and coating methods, are effective. However, surface roughness plays an important role in the chemical phenomena, although the grain boundaries in the nanostructure coatings have increased, the mechanism of corrosion is generally recognised as uniform corrosion. But in presented microstructure coating, it was presented as a localised corrosion. On that basis, the corrosion resistance of the surfaces of the tested materials was specified, depending on the heat and treatment method (Figure 14). The polarisation curves showed that the investigated material revealed pitting corrosion, particularly dangerous for magnesium alloys. Thus, corrosion resistance in the investigated nanostructure coatings was determined better than in the corresponding microstructure ones. The presence of chloride in the obtained coatings should also be considered (Fig. 9); however, because of the escape of Cl

from the surface of the coating at high temperatures, the Cl content in deposited coatings at high temperatures is less than the measuring resolution. On the other hand, the high values of the density of the corrosion current as well as the shape of the anodic curves gave information about the velocity of the dissolution of the investigated coatings. From the results, a comparison between the corrosion resistance of heat-treated magnesium and aluminium alloys showed that the values obtained for aluminium alloys clearly indicate their better corrosion resistance (Figure 14).

Consequently, the corrosion rate measured as the corrosion current density increases with increasing potential and temperature. In addition, it is shown in Fig. 14 that at the low deposition potential ca. -1.60 [V] for the magnesium alloys, and -0.60 [V] for the aluminium alloy, the rate of corrosion is reduced, potential of corrosion is still negative, the slope of anode branch (β anode) is steep; therefore, the rate of corrosion is decreased. For a positive corrosion resistance potential, the corrosion process for both alloys is the highest and is sill increasing.
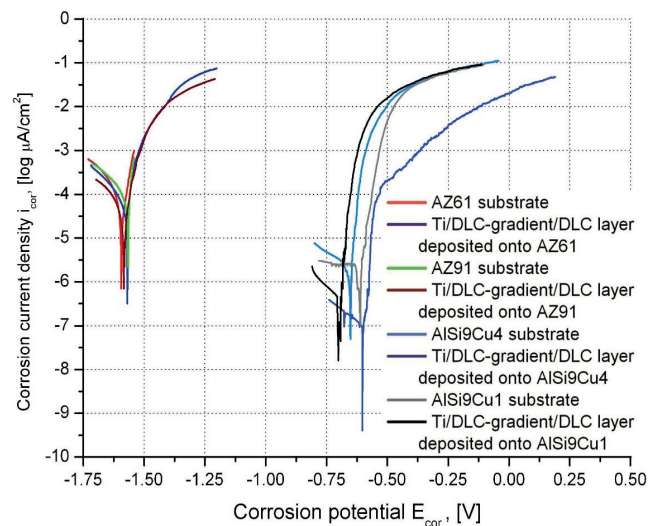

Fig. 14. Anodic polarisation curves registered for investigation alloys after heat and surface treatment

Such a relation is probably owed to the formation of a layer on the surface, effectively protecting against corrosion occurring in the material. The obtained corrosion resistance for the aluminium alloys was at a level of 9 $k\Omega cm^2$, roughly 1000 times higher than the value of polarisation resistance and it was characteristic of magnesium alloys. It determines the corrosion current density values, which were more than 100 times higher for magnesium than for aluminium alloys. The recorded test results of electrochemical corrosion analysed for the coating type Ti/DLC/DLC showed that the applied coating system effectively protects the surface of the tested alloys against pitting corrosion. However, the best results for the corrosion resistance for the DLC coating were obtained for the coated aluminium alloys, where a value was registered that was ~ 600 times higher than the polarisation resistance of coated magnesium alloys. Furthermore, polarisation resistance of the coated aluminium alloy ~ 120 $k\Omega cm^2$ was a few times higher than the polarisation resistance of the primary alloy ~ 35 $k\Omega cm^2$ after the standard heat treatment (Figure 15).

A higher corrosion resistance of DLC coating on the Al substrate is owed, and confirmed in metallographic research, to the high homogeneity of the obtained coatings and probably the occurrence of aluminium oxide film on the surface of Al alloys, resulting in a lower value of the corrosion potential of aluminium alloys.
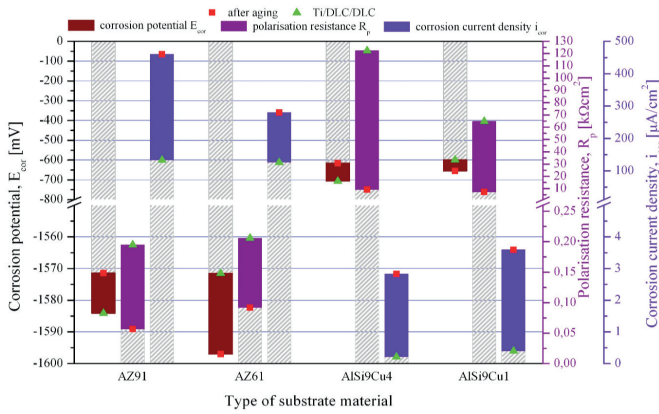

Fig. 15. Measurement results of corrosion current density i_{cor}; polarisation resistance R_p, corrosion potential E_{cor} of the surface of magnesium and aluminium cast alloys after ageing and chemical vapour deposition process

The identification of defects in the coatings resulting from the corrosion tests was based on an observation with a scanning confocal microscope and a stereoscopic light microscope. Pitting corrosion is generally defined as a type of localised corrosion because the effects are often generated during the corrosion progress and are invisible. The measured weight loss compared with the total corrosion is small, but over time it also leads to perforation of the surface, and thus, damage of the element.

Nucleation and growth of pits occur in the weakest areas of the passive layer (in places of potential corrosion) forming on the surface of metallic materials, in places with mechanical damage, near to precipitates, strengthening phases, pores, solidified drops of the deposited material, holes remaining after falling out drops, as well as at grain boundaries.

Metallographic investigations revealed open pitting corrosion places of different shapes (Figures 16-19) in the structure and surface of the cast magnesium and aluminium alloys, ranging from cylindrical to hemispherical. Such open corrosion places were relatively rare in the case of the investigated aluminium. At the bottom of the pitting holes, corrosion products resulting from dissolution of the tested material could be found because the surface acts as an anode, whereas the pitting environment acts as a cathode (Figure 20).
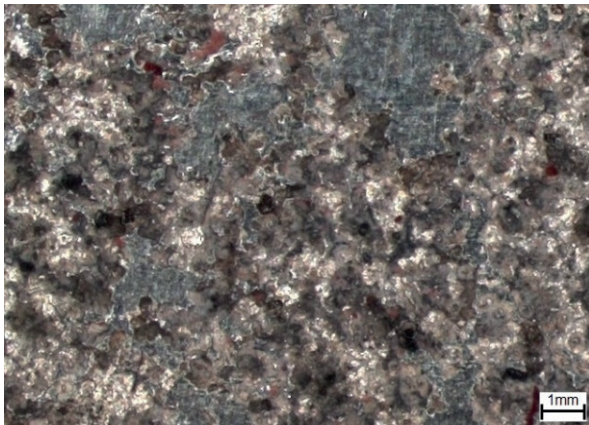

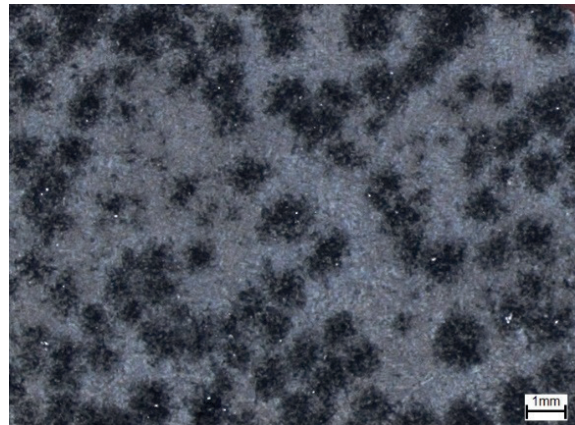Fig. 16. Surface structure of the magnesium cast alloy AZ61 after the corrosion test

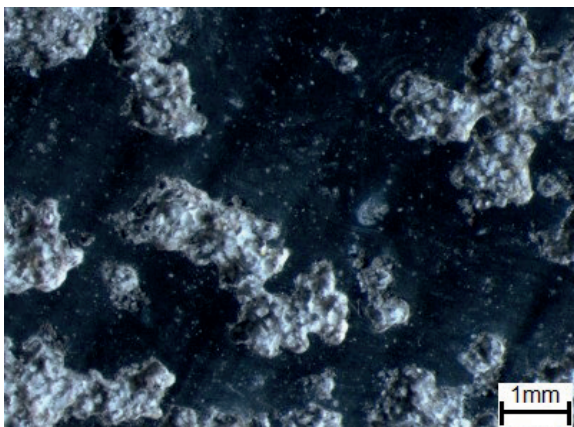Fig. 17. Surface structure of the magnesium cast alloy AlSi9Cu4 after the corrosion test

Fig. 18. Surface structure of the Ti/DLC/DLC coating deposited on the magnesium cast alloy AZ61 after the corrosion test, mag. 20x
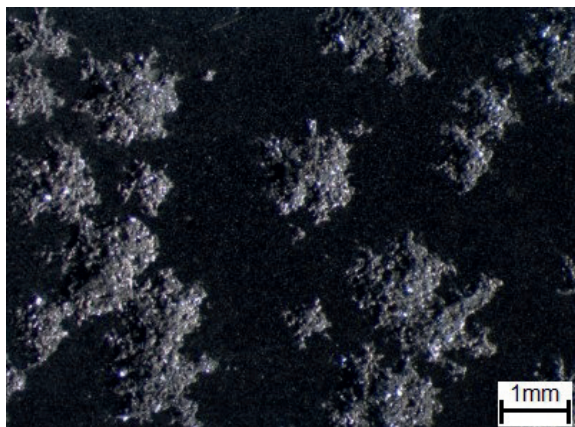

Fig. 19. Surface structure of the Ti/DLC/DLC coating deposited on the aluminium cast alloy AlSi9Cu1 after the corrosion test, mag. 20x
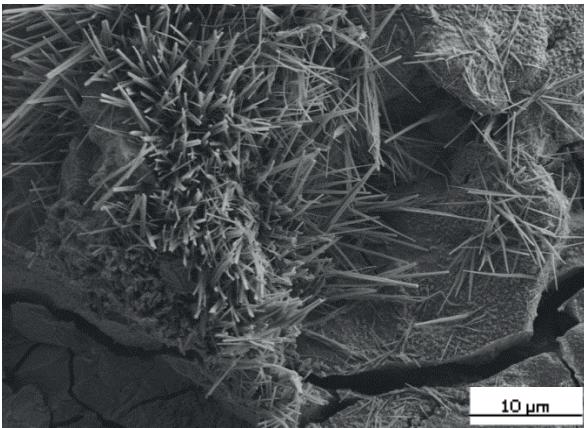
Fig. 20. Microstructure of the magnesium alloy AZ91 after corrosion tests (corrosion products)

4. Conclusion

The entire technological PACVD process takes place at temperatures of up to 180 °C because of the nature of the material used for investigations (Mg and Al alloys) and its relatively low melting point.

From the performed investigations, it was found that the deposited coatings did not reveal any delamination or defects and they closely adhere to each other. The thickness of the coating is in a range of up to 2.5 µm. Tests using transmission electron microscopy confirmed an amorphous character of low-friction DLC layers, especially based on the SAD diffraction techniques, where the ring-like character of the diffraction helps to determine the nature of the produced coating, together with exact determination of the d-spacing of the particular phase presented in the discussion part.

The highest corrosion resistance achieved for the DLC coating was obtained for the coated aluminium alloys, with a value 600 times higher compared to polarisation resistance, obtained for the DLC coating on magnesium alloys. The obtained investigations using Raman spectroscopy confirmed that the obtained DLC coating has a structure, which is non-ordered, where the ratio of the D1 band to the G band is an ordering measure of the carbon structure and the D3 band confirms the occurrence of the amorphous graphite fraction.

This amorphous graphite fraction with sp^3 hybridisation is responsible for enhancing the hardness of the obtained surface coating. The graphite fraction, also present in this type of coating, is responsible for the friction of the surface material, enabling such phenomena as self-lubrication and revealing a lower friction coefficient. The corrosion resistance investigation of the obtained coatings for the heat-treated magnesium and aluminium found that the values obtained for the investigated aluminium alloys had a much higher corrosion resistance potential than the magnesium cast alloys.

The highest value of the critical load was as high as L_{C1} - 7 N and L_{C2} - 19 N, and the highest adhesion of the coating on the substrate was achieved for the AZ91 magnesium alloy, close to the values of the other magnesium cast alloy AZ61 with critical load L_{C1} - 6 N and L_{C2} - 17 N. The best wear resistance test results were obtained for the magnesium alloy substrate - AZ61, for which the measured value of the friction path length was equal to 630 m.

REFERENCES

[1] E.F. Horst, B.L. Mordike, Magnesium Technology. Metallurgy, Design Data, Application, Springer-Verlag, Berlin Heidelberg 2006.

[2] J.G. Kauffman, E.L. Rooy, Aluminum Alloy Castings, ASM International, Ohio 2005.

[3] T. Tanski, Strojniski Vestnik-Journal of Mechanical Engineering 59, (3), 165-174 (2013), DOI: 10.5545/svjme.2012.522

[4] T. Tański, K. Labisz, K. Lukaszkowicz, A.Śliwa, K.Gołombek, Surface Engineering 30, (12), 27-932 (2014).

[5] L. Zeng, S. Yang, W. Zhang, Y. Guo, Ch. Yan, Electrochimica Acta. 55, (9), 3376-3383 (2010).

[6] Y.S. Zou, Y.F. Wu, H. Yang, K. Cang, G.H. Song, Z.X.Li, K. Zhou, Appl Surf Sci. 258, (4) 1624-1629 (2011).

[7] G. Wu, W. Dai, H. Zheng, A. Wang, Surface and Coatings Technology 205, (7), 2067-2073 (2010).

[8] G.R. dos Santos, D.D. da Costa, F.L. Amorim, R.D. Torres, Surface and Coatings Technology 202, (4), 1029–1033 (2007).

[9] A. Śliwa, J. Mikuła. K. Gołombek, T. Tański, W. Kwaśny, M. Bonek, Z. Brytan, Applied Surface Science, doi:10.1016/j. apsusc.2016.01.090.

[10] L.A. Dobrzański, M. Staszuk, K. Gołombek, A. Śliwa, M. Pancielejko, Arch Metall Mater. 55, (1), 187-193 (2010).

[11] K. Lukaszkowicz, J. Sondor, A. Kriz, M. Pancielejko, J Mater Sci. 45, (6), 1629-1637 (2010).

[12] L.A. Dobrzański, L. W. Żukowska, J. Mikuła, K. Gołombek, D.Pakuła, M. Pancielejko, J Mater Process Tech. 201, (1-3), 310-314 (2008).

[13] L.A. Dobrzański, K. Gołombek, J Mater Process Tech. 164-165, 805-815 (2005).

[14] J. Smolik, J.Walkowicz, T. Szubrycht, Surface and Coatings Technology. 174-175, 345-350 (2003).

[15] C.L. Chang, D.Y. Wang, Diam Relat Mater. 10, (8), 1528-1534 (2001).

[16] A. Matuszewska, R. Michalczewski, M. Grądkowski, M. Szczerek, Scientific Problems of Machines Operation and Maintenance. 150, (2), 31-40 (2007).

[17] Q. Wang, F. Zhou, Z. Zhou, Y. Yang, C. Yan, C. Wang, W. Zhang, L. Kwok-Yan Li, I. Bello, S. Tong Lee, Diam Relat Mater. 25, 163–175 (2012).

[18] J. Robertson, Material Science and Engineering R. 37, (4-6), 129-282 (2002).

[19] M. Basiaga, M. Staszuk, W. Walke, Z. Opilski, Materialwissenschaft Und Werkstofftechnik 47, (5-6), 512-520 (2016).

[20] E. Torres, D. Ugues, Z. Brytan, M. Perucca, J Phys D-App Phys. 42, (10), 2009.